Excellent Performance of One-Pot Synthesized Cu-SSZ-13 Catalyst for the Selective Catalytic Reduction of NO$_x$ with NH$_3$

Lijuan Xie,[†] Fudong Liu,[†] Limin Ren,[‡] Xiaoyan Shi,[†] Feng-Shou Xiao,[§] and Hong He*[,†]

[†]Research Center for Eco-Environmental Sciences, Chinese Academy of Sciences, Beijing 100085, China

[‡]College of Chemistry and State Key Laboratory of Inorganic Synthesis and Preparative Chemistry, Jilin University, Changchun 130012, China

[§]Department of Chemistry, Zhejiang University, Hangzhou 310028, China

Ⓢ Supporting Information

ABSTRACT: Cu-SSZ-13 samples prepared by a novel one-pot synthesis method achieved excellent NH$_3$−SCR performance and high N$_2$ selectivity from 150 to 550 °C after ion exchange treatments. The selected Cu$_{3.8}$-SSZ-13 catalyst was highly resistant to large space velocity (800 000 h^{-1}) and also maintained high NO$_x$ conversion in the presence of CO$_2$, H$_2$O, and C$_3$H$_6$ in the simulated diesel exhaust. Isolated Cu^{2+} ions located in three different sites were responsible for its excellent NH$_3$−SCR activity. Primary results suggest that the one-pot synthesized Cu-SSZ-13 catalyst is a promising candidate as an NH$_3$−SCR catalyst for the NO$_x$ abatement from diesel vehicles.
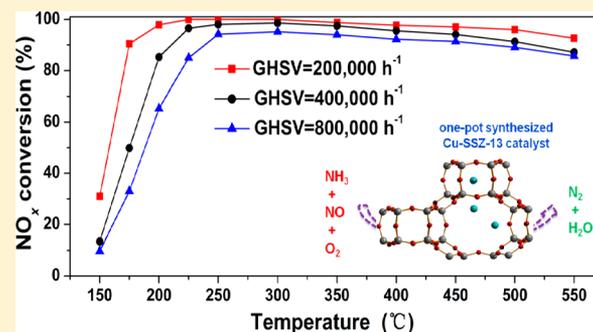
1. INTRODUCTION

Nitrogen oxides (NO$_x$), which result from automobile exhaust gas and industrial combustion of fossil fuels, is a major source of air pollution and can cause a series of environmental issues, such as photochemical smog and fine particle pollution (haze). Nowadays, the abatement of NO$_x$ from diesel engines in oxygen-rich conditions remains a challenge in the field of environmental catalysis. The selective catalytic reduction of NO$_x$ with NH$_3$ (NH$_3$−SCR) is one of the most promising technologies for NO$_x$ emission control from diesel engine exhaust. WO$_3$ or MoO$_3$ promoted V$_2$O$_5$/TiO$_2$ catalysts and zeolite-supported base metal (e.g., Cu, Fe) catalysts are commonly used in SCR after-treatment converters to meet the diesel NO$_x$ emission standards in the world.[1−3] A typical diesel emission control system using SCR also includes a diesel particulate filter (DPF) which may expose the SCR catalysts to high temperatures (>650 °C) during its regeneration.[4] Traditional vanadium-based catalysts cannot remain active in such a temperature range due to the phase transformation of the TiO$_2$ support. The toxicity of V$_2$O$_5$ to human health and the eco-environment is another important concern for its broad application on diesel engines. Although Fe-ZSM-5 and Cu-ZSM-5 catalysts have been investigated extensively in recent years, some serious problems still remain to be resolved. For instance, on one hand, the activity of Fe-ZSM-5 in the low temperature range and the activity of Cu-ZSM-5 in the high temperature range need to be further increased.[5] On the other hand, their activity always decreases significantly in the presence of water vapor at high temperatures due to the occurrence of dealumination, collapse of the zeolite structure, alteration of active metal species, and sintering of active

metals.[6−9] Additionally, zeolite catalysts using ZSM-5 as support are sensitive to hydrocarbon poisoning owing to their intrinsically large pores and cages (∼5.5 Å, ten-membered-ring), which are accessible to hydrocarbon deposition and coke formation.[10−12] Therefore, it is imperative to develop improved catalyst materials with excellent NH$_3$−SCR activity, high hydrothermal stability, and outstanding hydrocarbon poisoning resistance. Only such catalyst systems are qualified to respond to more stringent NO$_x$ emission limits.

Recently, Cu/zeolite catalysts with chabazite (CHA) crystal structure became a promising candidate for NH$_3$−SCR reaction, such as Cu-SAPO-34 and Cu-SSZ-13.[13−15] Cu-SSZ-13 prepared by an ion-exchange method showed improved activity, N$_2$ selectivity, and hydrothermal stability compared with existing Cu-zeolite catalysts, including Cu-ZSM-5, Cu-Y, and Cu-beta. It achieved excellent NO$_x$ conversion over the wide temperature range of 250−550 °C, and the activity was maintained even after severe hydrothermal treatment at 800 °C for 16 h.[8,9,16,17] CHA structure contained eight-membered-ring pores (3.8 × 3.8 Å) composed of six-membered rings in an AABBCC sequence. Such a small pore structure was expected to be more resistant to hydrocarbon poisoning.[8] Isolated Cu^{2+} species located in the six-membered rings were confirmed to be the active sites in the NH$_3$−SCR reaction over Cu-SSZ-13 catalyst.[18−20] Kwak proposed that Cu ions occupied sites in the large cages of the CHA structure at high ion exchange levels,

making them more easily reduced.[2] Compared with other Cu/zeolites, Cu-SSZ-13 maintained the zeolite structure well and the active species maintained unchanged after severe hydrothermal aging.[9] These characteristics indicate that a catalyst with such a structure could be a very promising candidate for practical application in NO_x emission control from diesel engines. However, the synthesis method of SSZ-13 zeolite reported by Zones in 1985 requires the very costly structure-directing agent *N,N,N*-trimethyl-1-adamantammonium hydroxide (TMAdaOH),[21,22] limiting the wide application of this material as a catalyst support. Therefore, it is desirable to improve the synthesis method to reduce the cost of Cu-SSZ-13 catalyst for the NH_3−SCR process. More recently, Ren et al. designed a one-pot synthesis method of Cu-SSZ-13 catalyst using low-cost copper-tetraethylenepentamine (Cu-TEPA) as a novel template, which is beneficial to the wide use of Cu-SSZ-13 catalyst.[23] The product achieves high Cu loading and high dispersion of Cu species simultaneously. Compared with the conventional ion exchange method, the direct route introducing Cu^{2+} species into the zeolites greatly enhanced the efficiency of Cu species. More importantly, the obtained catalyst exhibits good NH_3−SCR activity especially in the low temperature range. However, the activity needs to be further improved and much more work should be done to investigate this catalyst material in detail before its actual industrial application. In this study, we have further improved the synthesis method of Cu-SSZ-13 catalyst and systemically investigated its catalytic performance in the NH_3−SCR reaction under different working conditions. The improved method decreases the cost further and the optimal catalyst shows much better activity than the catalyst we have reported previously.[23] The results suggest that the one-pot synthesized Cu-SSZ-13 catalyst is a promising candidate for the $deNO_x$ process of diesel engines.

2. EXPERIMENTAL METHODS

2.1. Catalyst Preparation. The catalyst was synthesized according to a procedure similar to that used for Cu-ZJM-1-10 as reported by Ren.[23] Differently in this study, we adjusted the aluminosilicate gels to the mole ratio $14.8Na_2O:3.0Al_2O_3:600H_2O:30SiO_2:4Cu$-TEPA, using smaller amounts of reagents (the amount of Cu-TEPA was reduced to 2/3 of the original recipe) to obtain CHA structure. Cu source of Cu-TEPA was $CuSO_4 \cdot 5H_2O$. After crystallization at 140 °C for 4 days, the initial Cu-SSZ-13 product was obtained. Because the Cu content in the initial product was relatively high, an ion exchange method using NH_4NO_3 solution (1 mol/L) was applied to obtain suitable Cu loadings. After ion exchange for 5 h once and twice, we obtained two Cu-SSZ-13 samples with different Cu loadings. Then, all samples were calcined at 600 °C for 6 h to remove the residual templates and denoted as Cu_x-SSZ-13, where "x" represents the Cu content in the catalyst by weight. The hydrothermal treatment of optimal catalyst was carried out with a gas condition of air and 10% H_2O at 750 °C for 16 h.

2.2. NH_3−SCR Activity Measurement. SCR activity tests of the sieved powder catalysts were carried out in a fixed-bed quartz flow reactor at atmospheric pressure. The reaction conditions were controlled as follows: 500 ppm NO, 500 ppm NH_3, 5 vol % O_2, 5 vol % CO_2 (when used), 5 vol % H_2O (when used), 500 ppm C_3H_6 (when used), balance N_2, and 500 mL/min total flow rate. Different gas hourly space velocities (GHSVs) were obtained by changing the volume of catalysts. The effluent gas including NO, NH_3, NO_2, and N_2O was

continuously analyzed by an online NEXUS 670-FTIR spectrometer equipped with a heated, low volume (0.2 L) multiple-path gas cell (2 m). The FTIR spectra were collected throughout and the results were recorded when the SCR reaction reached a steady state. Then, the NO_x conversion and N_2 selectivity were calculated accordingly.

$$NO_x \text{ conversion} = \left(1 - \frac{[NO]_{out} + [NO_2]_{out}}{[NO]_{in} + [NO_2]_{in}}\right) \times 100\% \tag{1}$$

$$\begin{aligned} N_2 &\text{ selectivity} \\ &= \frac{[NO]_{in} + [NH_3]_{in} - [NO_2]_{out} - 2[N_2O]_{out}}{[NO]_{in} + [NH_3]_{in}} \\ &\times 100\% \end{aligned} \tag{2}$$

2.3. Catalyst Characterization. The specific surface area and pore volume of Cu-SSZ-13 serial catalysts were obtained from N_2 adsorption/desorption analysis at 77 K using a Quantachrome Quadrasorb SI-MP. Prior to the N_2 physisorption, all samples were degassed at 300 °C for 5 h. Micropore surface areas and micropore volumes were determined by *t*-plot method.

Powder X-ray diffraction (XRD) measurements were carried out on a computerized PANalytical X'Pert Pro diffractometer with Cu Kα (λ = 0.15406 nm) radiation. The data of 2θ from 5° to 40° were collected with the step size of 0.02°.

The Cu contents of the catalysts were analyzed using an inductively coupled plasma instrument (OPTMIA 2000DV) with a radial view of the plasma. All samples were dissolved using strong acid solution before tested. The calibration solution was prepared using pure materials. The average of three atomic emission lines was used to determine the Cu contents in the catalysts.

The H_2-TPR experiments were carried out on a Micromeritics AutoChem 2920 chemisorption analyzer. The samples (50 mg) in a quartz reactor were pretreated at 500 °C in a flow of air (50 mL/min) for 1 h and cooled down to the room temperature. Then H_2-TPR was performed in 10 vol % H_2/Ar gas flow of 50 mL/min at a heating rate of 10 °C/min.

The EPR spectra of hydrated and dehydrated samples were recorded on a JEOL spectrometer at 123 K. The JES FS200 software and the special JEOL program were used for data analysis. The fresh sample was pretreated at 500 °C for 2 h in 20 vol % O_2/N_2 to prepare dehydrated sample. For measurement, all samples were placed into quartz tubes and evacuated in vacuum.

3. RESULTS AND DISCUSSION

3.1. Characterization of Catalysts. As shown in Figure 1, the initial Cu-SSZ-13 product exhibited the typical diffraction peaks of the CHA zeolite structure (2θ = 9.5°, 14.0°, 16.1°, 17.8°, 20.7°, and 25.0°) with a good degree of crystallization.[24] The diffraction peaks for CuO (2θ = 35.6° and 38.8°) and Cu_2O (2θ = 36.44°) could not be identified. Therefore, the Cu species were dispersed very well in the initial Cu-SSZ-13 product. However, after calcination at 600 °C, the diffraction peaks of CuO were clearly observed. This phenomenon indicates that the Cu loading was too high in the initial product, showing cations migration and transformation during the thermal treatment process. After treatment in NH_4NO_3 solution for 5 h once and twice and then calcination at 600 °C,
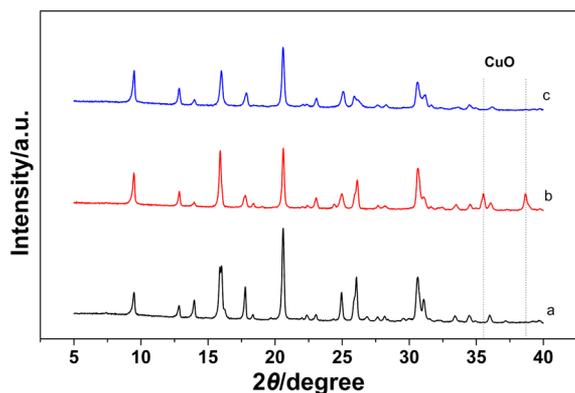
Figure 1. XRD patterns of the one-pot synthesized initial product and Cu$_x$-SSZ-13 catalyst: (a) Initial product, (b) Cu$_{10.3}$-SSZ-13, (c) Cu$_{3.8}$-SSZ-13.

the Cu loading of the catalyst decreased from 10.3 wt % to 3.8 wt % and 3.6 wt %, respectively, and Na content decreased from 4.6 wt % to 1.2 wt % and 0.7 wt %, respectively (shown in Table 1). The diffraction peaks for CuO also disappeared in the

Table 1. Physicochemical Properties of Cu$_x$-SSZ-13 Catalysts

catalysts	S_{micro} (m^2/g)	V_{micro} (cm^3/g)	Si/Al$_2$ ratio	Cu content (wt %)	Na content (wt %)
Cu$_{10.3}$-SSZ-13	477.5	0.23	8.3	10.3	4.6
Cu$_{3.8}$-SSZ-13	525.7	0.26	8.3	3.8	1.2
Cu$_{3.6}$-SSZ-13	528.2	0.26	8.3	3.6	0.7

XRD profile, because of removal of Cu outside of cages. The formation of CuO in Cu-zeolite catalysts has been an important reason for the decrease of NO$_x$ conversion in the high temperature range due to the occurrence of unselective catalytic oxidation of NH$_3$ to NO$_x$ in NH$_3$−SCR process, which was demonstrated in previous studies.[7] Therefore, the ion exchange treatment was very necessary to obtain Cu-SSZ-13 catalysts with appropriate Cu loadings in our study.

The results of the specific surface areas and pore volumes derived from N$_2$ physisorption are summarized in Table 1. Compared with Cu$_{10.3}$-SSZ-13, the surface area and pore volume of Cu$_{3.8}$-SSZ-13 increased from 477.5 to 525.7 m^2/g and 0.23 to 0.26 cm^3/g, respectively. This increase should be associated with the disappearance of CuO, which could block the pores of the SSZ-13 zeolite. It is noteworthy that there was no distinct difference in surface area and pore volume between Cu$_{3.8}$-SSZ-13 and Cu$_{3.6}$-SSZ-13 with similar Cu loading, although the latter catalyst was ion exchanged by NH$_4$NO$_3$ twice, indicating that one-time ion exchange was completely sufficient for the elimination of excess Cu species from the SSZ-13 zeolite structure.

3.2. NH$_3$−SCR Performance of Catalysts under Different Reaction Conditions. NO$_x$ conversion as a function of reaction temperature between 150 and 550 °C over Cu-SSZ-13 catalysts with different Cu loadings is shown in Figure 2. During the performance tests, about 50 mg catalyst was used, yielding a rather high GHSV of 400 000 h^{-1}. The Cu$_{10.3}$-SSZ-13 catalyst with the highest Cu loading exhibited the lowest performance compared with the others. Because of the formation of CuO, the NO$_x$ conversion decreased rapidly
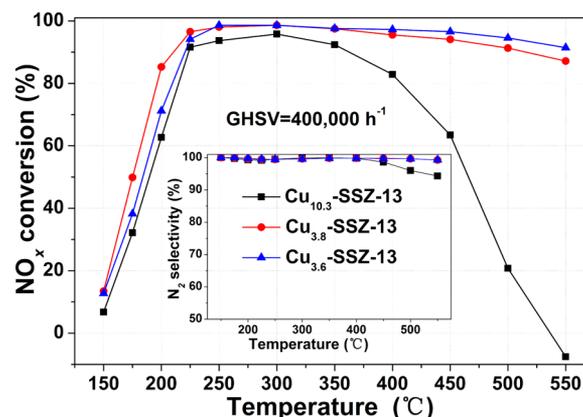
Figure 2. NO$_x$ conversions and N$_2$ selectivity over Cu$_x$-SSZ-13 catalysts.

when the temperature was above 400 °C. CuO was unrelated to the SCR activity in the low temperature range, and decreased the activity in the high temperature range seriously due to the overoxidation of NH$_3$.[25,26] Thus, elimination of CuO was necessary to prepare better catalysts. For Cu$_{3.8}$-SSZ-13 with appropriate Cu loading, the NO$_x$ conversion was further improved over the whole temperature range, reaching *ca.* 85% at 200 °C and maintaining a level above 90% until 550 °C. For the Cu$_{3.6}$-SSZ-13 catalyst with Cu content similar to Cu$_{3.8}$-SSZ-13, a slight decline was observed in the SCR performance over the whole temperature range. Furthermore, excellent N$_2$ selectivity over both Cu$_{3.8}$-SSZ-13 and Cu$_{3.6}$-SSZ-13 catalysts could be obtained, at nearly 100% from 150 to 550 °C and relatively higher than that over the Cu$_{10.3}$-SSZ-13 catalyst. In short, the ion exchange by NH$_4$NO$_3$ is an important treatment procedure for obtaining an excellent Cu-SSZ-13 catalyst with high SCR performance and N$_2$ selectivity simultaneously, and one-time exchange is sufficient to produce a suitable catalyst for the NH$_3$−SCR reaction. Additionally, deNO$_x$ catalytic activities of Cu$_{3.8}$-SSZ-13 catalyst at 600, 650, and 700 °C were also tested because the instantaneous temperature can be up to 600−700 °C in the real diesel exhaust (Table S1). The results indicate that the catalyst could also maintain good NH$_3$−SCR performance in such a high temperature range. Figure 3 shows the NO$_x$ conversions over the Cu$_{3.8}$-SSZ-13 catalyst under
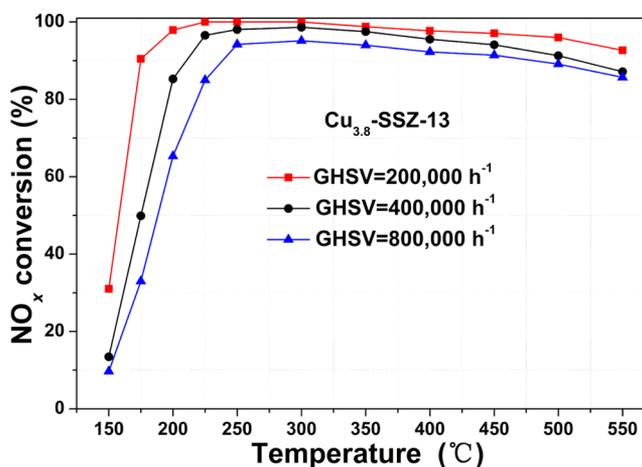
Figure 3. NO$_x$ conversions over Cu$_{3.8}$-SSZ-13 catalyst under different GHSVs.

different GHSVs. It is clear that the increase of GHSV from 200 000 to 400 000 h^{-1} resulted in the decrease of NH$_3$−SCR performance to a certain extent at low temperatures especially below 200 °C, yet there was no distinct effect on the high temperature SCR performance. Remarkably, the Cu$_{3.8}$-SSZ-13 catalyst showed rather high NO$_x$ conversions exceeding 90% within a broad operation temperature window from 250 to 550 °C even under an extremely high GHSV of 800 000 h^{-1}, suggesting that this catalyst is highly resistant to the effects of large space velocity. This characteristic is crucial for its practical application in diesel vehicles with limited installation space on board for a SCR after-treatment converter.

As the composition of diesel exhaust is complicated, we further tested the NH$_3$−SCR performance of the Cu$_{3.8}$-SSZ-13 catalyst in the presence of CO$_2$, H$_2$O, and C$_3$H$_6$ under the GHSV of 400 000 h^{-1}, with the results shown in Figure 4.
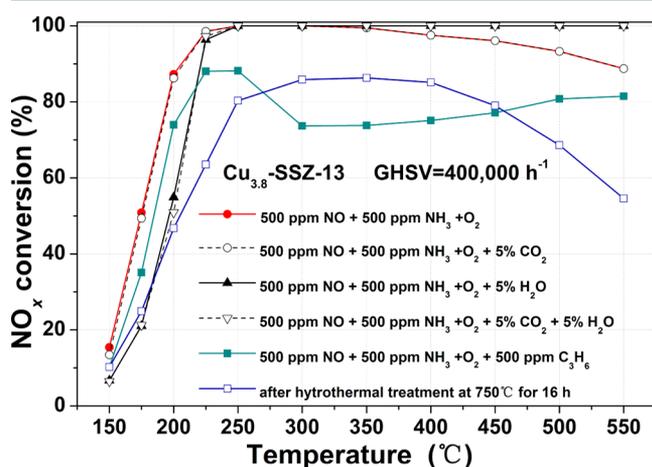
Figure 4. NO$_x$ conversions over Cu$_{3.8}$-SSZ-13 catalyst under different reaction conditions.

There was no inhibition effect on NH$_3$−SCR performance observed at all when 5% CO$_2$ was present in the feed gas. By comparison, the presence of 5% H$_2$O decreased the NO$_x$ conversion significantly at low temperatures (<200 °C) mainly due to the competitive adsorption by H$_2$O adsorption and increased the NO$_x$ conversion at high temperatures (>400 °C) probably due to the inhibition effect of H$_2$O on the unselective catalytic oxidation of NH$_3$.[27,28] It was also demonstrated that there was no synergistic inhibition effect on SCR performance in the coexistence of CO$_2$ and H$_2$O. The presence of 500 ppm C$_3$H$_6$ inhibited the NH$_3$−SCR reactions especially around 300 °C, probably due to the partial oxidation of C$_3$H$_6$ (Figure S1).[10] The NO$_x$ conversion increased in the high temperature range at around 400 °C, which should be related to the occurrence of HC-SCR during the NH$_3$−SCR reaction (Figure S2).[11,19] Compared with other Cu/zeolites and Fe/zeolites, Cu-SSZ-13 exhibits better C$_3$H$_6$ poisoning resistance.[11,29] After hydrothermal treatment at 750 °C for 16 h, the NO$_x$ conversion maintained higher than 80% from 250 to 450 °C, indicating its good hydrothermal stability. The XRD profile of aged Cu$_{3.8}$-SSZ-13 sample showed that the CHA structure was still maintained, although a small amount of amorphous phase appeared (Figure S3). Both the structural stability of the zeolite and the Cu species stability could affect the hydrothermal stability of the catalyst. It is well-known that the bonds of Si−O−Al were less stable than those of Si−O−Si and dealumination occurred via attack of Si−O−Al by H$_2$O.[6] The

damage of structure aroused by dealumination was fatal for catalysts.[27] Al NMR profile of aged Cu$_{3.8}$-SSZ-13 sample indicated the occurrence of dealumination during the hydrothermal treatment (Figure S4), which should be the main reason for its decreased NO conversion. Thus, it is positive to improve the Si/Al$_2$ ratio for further improvement of the hydrothermal stability of the catalyst. The influence of Cu species stability will be discussed below.

3.3. Distribution of Cu Species in Cu-SSZ-13 Catalyst. H$_2$-TPR profiles of Cu$_{10.3}$-SSZ-13, Cu$_{3.8}$-SSZ-13, and Cu$_{3.6}$-SSZ-13 are shown in Figure 5a. No H$_2$ consumption could be
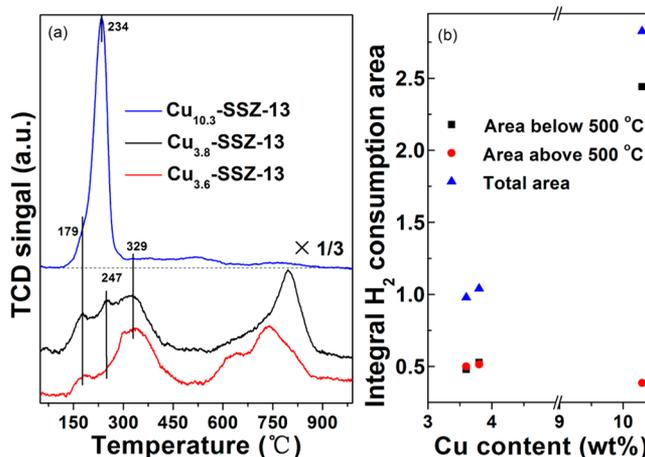
Figure 5. H$_2$-TPR profiles of Cu$_{10.3}$-SSZ-13, Cu$_{3.8}$-SSZ-13, and Cu$_{3.6}$-SSZ-13 catalysts (a); integrated H$_2$ consumption areas as a function of Cu loading in different temperature range (b).

observed for H-SSZ-13 (Figure S5), which proved that all H$_2$ consumption peaks in the H$_2$-TPR profiles of Cu-SSZ-13 catalysts were due to the reduction of Cu species. H$_2$-TPR is an effective method to identify dimeric and CuO cluster from isolated Cu^{2+} due to the more facile reduction of them. In previous studies, the one-step reduction of dispersed bulk CuO to Cu^0 occurred in the temperature range (200−300 °C).[30] Similar with CuO, [Cu−O−Cu]$^{2+}$ dimers also could be reduced to Cu^0 in the temperature range below 800 K.[31] Differently, reduction of isolated Cu^{2+} in zeolites has been proposed to occur by a two-step mechanism, namely, the reduction from Cu^{2+} to Cu$^+$ (at low temperatures) and the reduction from Cu$^+$ to Cu^0 (>800 K).[32] Thus, the H$_2$ consumption areas below 500 °C and the areas above 500 °C were calculated for all three catalysts. As shown in Figure 5b, a very large amount of H$_2$ consumption area was observed below 500 °C for Cu$_{10.3}$-SSZ-13 catalyst, suggesting that not only the reduction from Cu^{2+} to Cu$^+$ but also the reduction from Cu$^+$ to Cu^0 occurred before 500 °C. The XRD pattern proved the existence of CuO in the Cu$_{10.3}$-SSZ-13 catalyst (Figure 1). Therefore, the large peak at 234 °C observed for the Cu$_{10.3}$-SSZ-13 catalyst should be caused by the dispersed CuO to a large extent. However, the integral H$_2$ consumption areas below and above 500 °C were equal for both Cu$_{3.8}$-SSZ-13 and Cu$_{3.6}$-SSZ-13 catalysts (Figure 5b), meaning no Cu^0 formed below 500 °C. Thus, the existence of CuO or [Cu−O−Cu]$^{2+}$ dimers were excluded safely, and only isolated Cu^{2+} existed in the two catalysts. Therefore, three apparent reduction peaks (ca. 179, 247, and 329 °C) for the Cu$_{3.8}$-SSZ-13 catalyst could be assigned to the reduction of isolated Cu^{2+} to Cu$^+$. The easy reducibility of isolated Cu^{2+} ions (the reduction temperature

was as low as 179 °C) was responsible for the excellent NH_3–SCR performance in the low temperature range.

It is well-known that there are four types of cationic sites in chabazite. Site I is displaced from the six-membered-ring into the ellipsoidal cavity. Site II is located near the center of the ellipsoidal cavity. Site III is located in the center of the hexagonal prism. Site IV is located near the eight-membered-ring window.[33,34] Isolated Cu^{2+} ions locating at different cationic sites should show different H_2 reduction temperatures. In order to better assign the reduction peaks, EPR experiments were carried out for the selective $Cu_{3.8}$-SSZ-13 catalyst. EPR was an excellent technique for identifying the coordination environment of isolated Cu^{2+} ions, because all the other Cu species (Cu–O–Cu or Cu^+) were EPR silent.[34,35] Both EPR spectra of hydrated and dehydrated $Cu_{3.8}$-SSZ-13 samples were collected in this study (Figure 6a).
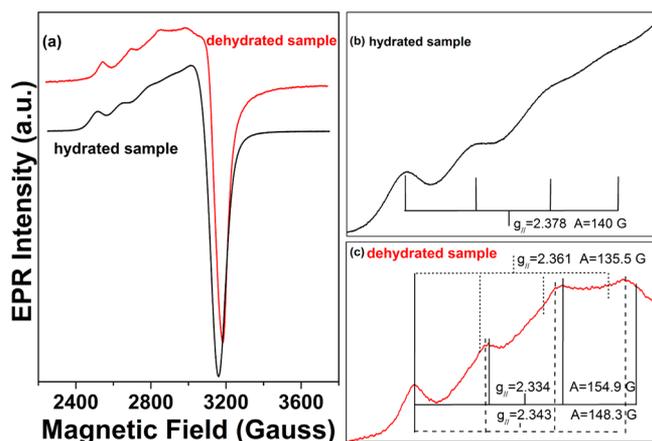
Figure 6. EPR spectra of $Cu_{3.8}$-SSZ-13 catalyst recorded at 123 K. (a) Hydrated sample (dark line) and dehydrated sample (red line). Analysis of the hyperfine features of hydrated sample (b) and dehydrated sample (c).

By analyzing the hyperfine features of the hydrated sample (Figure 6b), $g_{//}$ = 2.378 and A = 140 G was obtained. Zamadics et al. reported that EPR signal ($g_{//}$ = 2.381, A = 143 G) in hydrated Cu-SAPO-34 could be assigned to Cu^{2+} located in site I as a complex $Cu(O_F)_3(H_2O)_3$.[34] The similar EPR signals for Cu-CHA catalysts reported by others were also suggested to be this type of species, such as $g_{//}$ = 2.39 with A = 111 G and $g_{//}$ = 2.394 with A = 131 G.[25,31] Thus, this EPR signal should be due to the isolated Cu^{2+} located in site I for hydrated $Cu_{3.8}$-SSZ-13 catalyst (Cu^{2+}_I).[34,31] Because isolated Cu^{2+} species could migrate from one site to another upon thermal treatment, the dehydrated sample always contained more types of Cu species than the hydrated sample.[34] The similar phenomenon was also observed for the $Cu_{3.8}$-SSZ-13 catalyst, and three distinct Cu^{2+} species were discovered from the three sets of parameters determined from the EPR signal for the dehydrated sample (Figure 6c). Narayana et al. reported that the Cu^{2+} in site I with trigonal environment for dehydrated sample showed EPR signal of $g_{//}$ = 2.379 with A = 133 G.[36] In addition, Herman et al. proved that EPR signals of Cu^{2+} with trigonal environment varied with different Cu loading and different evacuation time in dehydration process, and the signals from $g_{//}$ = 2.36 with A = 125 G to $g_{//}$ = 2.38 with A = 110 G were recorded.[37] Thus, the first species for dehydrated sample giving rise to the $g_{//}$ = 2.361

and A = 135.5 G (Figure 6c) in $Cu_{3.8}$-SSZ-13 could be assigned to Cu^{2+} located in site I (Cu^{2+}_I).[34,36]

Yu et al. reported that the species located in hexagonal prism (site III) showed EPR single at $g_{//}$ = 2.335 with A = 155 G base on a lack of oxygen broadening.[38] Zamadics et al. also assigned the EPR single of $g_{//}$ = 2.336 with A = 168 G to Cu species in site III.[34] Thus, the second species with $g_{//}$ = 2.334 and A = 154.9 G in this study could be assigned to isolated Cu^{2+} species located in site III (Cu^{2+}_{III}).[34] Xue et al. proved that the H_2 reduction peak at *ca.* 250−260 °C was aroused from Cu^{2+}_I perfectly.[25] Thus, the H_2 reduction peak at 247 °C was attributed to Cu^{2+}_I. Isolated Cu^{2+} ions locating in site III with higher coordination number, which are more difficult to be reduce, are more stable than the Cu^{2+} ions locating in site I.[2] Thus, the reduction peak at 329 °C should be caused by the Cu^{2+}_{III}. Besides of Cu^{2+} species locating in the sites I and III, the third Cu^{2+} species with $g_{//}$ = 2.343 and A = 148.3 G could occupy site II or IV in the chabizite structure. However, site II is occupied only in hydrated chabazite.[33,40] Thus, the third type of species could be assigned to the isolated Cu^{2+} locating in site IV. It was reported that the isolated Cu^{2+} ions occupying site IV were much easier to reduce than those locating in site I; therefore, it is reasonable that the reduction peak at ca. 179 °C is caused by isolated Cu^{2+} ions in site IV (Cu^{2+}_{IV}).[2,41] In summary, the H_2 reduction peaks at 179, 247, and 329 °C for dehydrated $Cu_{3.8}$-SSZ-13 catalyst were attributed to isolated Cu^{2+} ions locating in site IV, I, and III of chabizite structure, respectively.

It is known that Cu^{2+} species located in site III was less active than species in site I in NH_3–SCR reaction due to steric hindrance.[39] The conclusion is proven in this study, as shown below. Figure 5 shows that the distribution of Cu species was changed during the second NH_4NO_3 treatment. More Cu^{2+}_{III} species were observed in $Cu_{3.6}$-SSZ-13 than $Cu_{3.8}$-SSZ-13 from H_2-TPR profiles, and poorer activity was observed in the low temperature range for $Cu_{3.6}$-SSZ-13 catalyst (Figure 2). Thus, the ratio of (Cu^{2+}_I + Cu^{2+}_{IV})/Cu^{2+}_{III} play an important role for NH_3–SCR reaction over Cu-SSZ-13 catalyst prepared by one-pot synthesis method. It was reported that the reduction of Cu^+ species to Cu^0 was expected when the CHA structure begin to degrade.[31] The higher reduction temperature from Cu^+ to Cu^0 represents the better stability of the species. Compared with $Cu_{3.8}$-SSZ-13, the reduction temperature was much lower for $Cu_{3.6}$-SSZ-13 catalyst (Figure 5). The NH_3–SCR performance of aged $Cu_{3.6}$-SSZ-13 catalyst was much poorer (Figure S6). Thus, the high hydrothermal stability of $Cu_{3.8}$-SSZ-13 catalyst is relative to its high stability of Cu species.

■ ASSOCIATED CONTENT

Ⓢ Supporting Information

NH_3–SCR activity at high temperatures, effect of C_3H_6,[27] Al NMR and XRD profiles for aged $Cu_{3.8}$-SSZ-13, NH_3–SCR activity of aged $Cu_{3.6}$-SSZ-13. This material is available free of charge via the Internet at http://pubs.acs.org.

■ AUTHOR INFORMATION

Corresponding Author

*Fax: +86 10 62849123; Tel: +86 10 62849123; E-mail: honghe@rcees.ac.cn.

Notes

The authors declare no competing financial interest.

■ REFERENCES

(1) Roy, S.; Hegde, M. S.; Madras, G. Catalysis for NO$_x$ abatement. *Appl. Energy* **2009**, *86* (11), 2283−2297.

(2) Kwak, J. H.; Zhu, H.; Lee, J. H.; Peden, C. H. F.; Szanyi, J. Two different cation positions in Cu-SSZ-13? *Chem. Commun.* **2012**, *48*, 4758−4760.

(3) Long, R. Q.; Yang, R. T. Reaction mechanism of selective catalytic reduction of NO with NH$_3$ over Fe-ZSM-5 catalyst. *J. Catal.* **2002**, *207* (2), 224−231.

(4) Kwak, J. H.; Tran, D.; Szanyi, J.; Peden, C. H. F.; Lee, J. H. The effect of copper loading on the selective catalytic reduction of nitric oxide by ammonia over Cu-SSZ-13. *Catal. Lett.* **2012**, *142* (3), 295−301.

(5) Kröcher, O.; Elsener, M. Combination of V$_2$O$_5$/WO$_3$-TiO$_2$, Fe-ZSM5, and Cu-ZSM5 catalysts for the selective catalytic reduction of nitric oxide with ammonia. *Ind. Eng. Chem. Res.* **2008**, *47* (22), 8588−8593.

(6) Sandro, B.; Oliver, K.; Arno, T.; Roderik, A. The state of the art in selective catalytic reduction of NO$_x$ by ammonia using metal-exchanged zeolite catalysts. *Catal. Rev.* **2008**, *50* (4), 492−531.

(7) Park, J.; Park, H.; Baik, J.; Nam, I.; Shin, C.; Lee, J.; Cho, B.; Oh, S. Hydrothermal stability of CuZSM5 catalyst in reducing NO by NH$_3$ for the urea selective catalytic reduction process. *J. Catal.* **2006**, *240* (1), 47−57.

(8) Fickel, D. W.; D'Addio, E.; Lauterbach, J. A.; Lobo, R. F. The ammonia selective catalytic reduction activity of copper-exchanged small-pore zeolites. *Appl. Catal., B* **2011**, *102* (3−4), 441−448.

(9) Kwak, J. H.; Tran, D.; Burton, S. D.; Szanyi, J.; Lee, J. H.; Peden, C. H. F. Effects of hydrothermal aging on NH$_3$-SCR reaction over Cu/zeolites. *J. Catal.* **2012**, *287*, 203−209.

(10) Heo, I.; Lee, Y.; Nam, I.-S.; Choung, J. W.; Lee, J.-H.; Kim, H.-J. Effect of hydrocarbon slip on NO removal activity of CuZSM5, FeZSM5 and V$_2$O$_5$/TiO$_2$ catalysts by NH$_3$. *Microporous Mesoporous Mater.* **2011**, *141* (1−3), 8−15.

(11) Sultana, A.; Nanba, T.; Sasaki, M.; Haneda, M.; Suzuki, K.; Hamada, H. Selective catalytic reduction of NO$_x$ with NH$_3$ over different copper exchanged zeolites in the presence of decane. *Catal. Today* **2011**, *164* (1), 495−499.

(12) Asima, S.; Tetsuya, N.; Masaaki, H.; Hideaki, H. SCR of NO$_x$ with NH$_3$ over Cu/NaZSM-5 and Cu/HZSM-5 in the presence of decane. *Catal. Commun.* **2009**, *10* (14), 1859−1863.

(13) Deka, U.; Lezcano-Gonzalez, I.; Warrender, S. J.; Picone, A. L.; Wright, P. A.; Weckhuysen, B. M.; Beale, A. M. Changing active sites in Cu-CHA catalysts: deNO$_x$ selectivity as a function of the preparation method. *Microporous Mesoporous Mater.* **2013**, *166*, 144−152.

(14) Raquel, M.-F.; Manuel, M.; Cristina, F.; Arkady, K.; Avelino, C. Rational direct synthesis methodology of very active and hydrothermally stable Cu-SAPO-34 molecular sieves for the SCR of NO$_x$. *Appl. Catal., B* **2012**, *127*, 273−280.

(15) Yang, X.; Wu, Z.; Moses-Debusk, M.; Mullins, D. R.; Mahurin, S. M.; Geiger, R. A.; Kidder, M.; Narula, C. K. Heterometal incorporation in metal-exchanged zeolites enables low-temperature catalytic activity of NO$_x$ reduction. *J. Phys. Chem. C* **2012**, *116* (44), 23322−23331.

(16) Kwak, J. H.; Tonkyn, R. G.; Kim, D. H.; Szanyi, J.; Peden, C. H. F. Excellent activity and selectivity of Cu-SSZ-13 in the selective catalytic reduction of NO$_x$ with NH$_3$. *J. Catal.* **2010**, *275* (2), 187−190.

(17) Schmieg, S. J.; Oh, S. H.; Kim, C. H.; Brown, D. B.; Lee, J. H.; Peden, C. H. F.; Kim, D. H. Thermal durability of Cu-CHA NH$_3$-SCR catalysts for diesel NO$_x$ reduction. *Catal. Today* **2011**, *184*, 252−261.

(18) Fickel, D. W.; Lobo, R. F. Copper coordination in Cu-SSZ-13 and Cu-SSZ-16 investigated by variable-temperature XRD. *J. Phys. Chem. C* **2010**, *114*, 1633−1640.

(19) Korhonen, S. T.; Fickel, D. W.; Lobo, R. F.; Weckhuysen, B. M.; Beale, A. M. Isolated Cu^{2+} ions: active sites for selective catalytic reduction of NO. *Chem. Commun.* **2011**, *47* (2), 800−802.

(20) Deka, U.; Juhin, A.; Eilertsen, E. A.; Emerich, H.; Green, M. A.; Korhonen, S. T.; Weckhuysen, B. M.; Beale, A. M. Confirmation of isolated Cu^{2+} ions in SSZ-13 zeolite as active sites in NH$_3$-selective catalytic reduction. *J. Phys. Chem. C* **2012**, *116* (7), 4809−4818.

(21) Zones, Zeolites SSZ-13 and its method of preparation; U.S. Patent 4544538, 1985.

(22) Zones, S. I. Conversion of faujasites to high-silica chabazite SSZ-13 in the presence of N,N,N-trimethyl-1-adamantammonium iodide. *J. Chem. Soc., Faraday Trans.* **1991**, *87* (22), 3709−3716.

(23) Ren, L.; Zhu, L.; Yang, C.; Chen, Y.; Sun, Q.; Zhang, H.; Li, C.; Nawaz, F.; Meng, X.; Xiao, F.-S. Designed copper-amine complex as an efficient template for one-pot synthesis of Cu-SSZ-13 zeolite with excellent activity for selective catalytic reduction of NO$_x$ by NH$_3$. *Chem. Commun.* **2011**, *47* (35), 9789−9791.

(24) Higgins, M. T. a. J. *Collection of simulated XRD patterns for zeolites*, 5th ed.; Elsevier: Amsterdam, 2007; pp 112−115.

(25) Xue, J.; Wang, X.; Qi, G.; Wang, J.; Shen, M.; Li, W. Characterization of copper species over Cu/SAPO-34 in selective catalytic reduction of NO$_x$ with ammonia: Relationships between active Cu sites and de-NO$_x$ performance at low temperature. *J. Catal.* **2013**, *297*, 56−64.

(26) Wang, L.; Li, W.; Qi, G.; Weng, D. Location and nature of Cu species in Cu/SAPO-34 for selective catalytic reduction of NO with NH$_3$. *J. Catal.* **2012**, *289*, 21−29.

(27) Sjövall, H.; Olsson, L.; Fridell, E.; Blint, R. J. Selective catalytic reduction of NO$_x$ with NH$_3$ over Cu-ZSM-5-The effect of changing the gas composition. *Appl. Catal., B* **2006**, *64* (3−4), 180−188.

(28) Li, J.; Chang, H.; Ma, L.; Hao, J.; Yang, R. T. Low-temperature selective catalytic reduction of NO$_x$ with NH$_3$ over metal oxide and zeolite catalysts-A review. *Catal. Today* **2011**, *175* (1), 147−156.

(29) Ma, L.; Li, J.; Cheng, Y.; Lambert, C. K.; Fu, L. Propene poisoning on three typical Fe-zeolites for SCR of NO$_x$ with NH$_3$: from mechanism study to coating modified architecture. *Environ. Sci. Technol.* **2012**, *46* (3), 1747−1754.

(30) Richter, M.; Fait, M.; Eckelt, R.; Schneider, M.; Radnik, J.; Heidemann, D.; Fricke, R. Gas-phase carbonylation of methanol to dimethyl carbonate on chloride-free Cu-precipitated zeolite Y at normal pressure. *J. Catal.* **2007**, *245* (1), 11−24.

(31) Gao, F.; Walter, E. D.; Karp, E. M.; Luo, J.; Tonkyn, R. G.; Kwak, J. H.; Szanyi, J.; Peden, C. H. F. Structure−activity relationships in NH$_3$-SCR over Cu-SSZ-13 as probed by reaction kinetics and EPR studies. *J. Catal.* **2013**, *300*, 20−29.

(32) Kefirov, R.; Penkova, A.; Hadjiivanov, K.; Dzwigaj, S.; Che, M. Stabilization of Cu$^+$ ions in BEA zeolite: Study by FTIR spectroscopy of adsorbed CO and TPR. *Microporous Mesoporous Mater.* **2008**, *116* (1−3), 180−187.

(33) Dědeček, J.; Wichterlová, B.; Kubát, P. Siting of the Cu$^+$ ions in dehydrated ion exchanged synthetic and natural chabasites: a Cu$^+$ photoluminescence study. *Microporous Mesoporous Mater.* **1999**, *32*, 63−74.

(34) Zamadies, M.; Chen, X.; Kevan, L. Study of copper(II) location and adsorbate interaction in CuH-SAPO-34 molecular sieve by electron spin resonance and electron spin echo modulation spectroscopies. *J. Phys. Chem.* **1992**, *96*, 2652−2657.

(35) Deka, U.; Lezcano-Gonzalez, I.; Weckhuysen, B. M.; Beale, A. M. Local environment and nature of Cu active sites in zeolite-based catalysts for the selective catalytic reduction of NO$_x$. *ACS Catal.* **2013**, *3* (3), 413−427.

(36) Narayana, M.; Kevan, L. Detection of a new trigonal bipyramidal copper species in Cu-CaX zeolite by electron spin resonance and electron spin echo modulation analysis. *J. Chem. Phys.* **1983**, *78* (6), 3573.

(37) Herman, R. G.; Flentgelb, D. R. Electron paramagnetic resonance parameters of copper (II) Y Zeolites. *J. Phys. Chem.* **1978**, *82* (6), 720−729.

(38) Yu, J.-S.; Ryoo, J. W.; Kim, S. J.; Hong, S. B.; Kevan, L. Cupric ion species in Cu(II)-exchanged K-Offretite gallosilicate determined by electron spin resonance and electron spin echo modulation spectroscopies. *J. Phys. Chem.* **1996**, *100*, 12624−12630.

(39) Wang, J.; Yu, T.; Wang, X.; Qi, G.; Xue, J.; Shen, M.; Li, W. The influence of silicon on the catalytic properties of Cu/SAPO-34 for NO$_x$ reduction by ammonia-SCR. *Appl. Catal., B* **2012**, *127*, 137−147.

(40) Calligaris, M.; Mezzetti, A.; Nardin, G.; Randaccio, L. Crystal structures of hydrated and dehydrated forms of a Mn(II)-exchanged chabazite. *Zeolites* **1985**, *5*, 317−319.

(41) Kieger, S. e.; Delahay, G. e.; Coq, B.; Neveu, B. Selective catalytic reduction of nitric oxide by ammonia over Cu-FAU catalysts in oxygen-rich atmosphere. *J. Catal.* **1999**, *183*, 267−280.